Journal of Physics: Conference Series **295** (2011) 012114 doi:10.1088/1742-6596/295/1/012114

Spin transfer coefficient D_{LL}^{Λ} to Λ hyperon in semi-inclusive DIS at HERMES

S Belostotski, D Veretennikov and Yu Naryshkin

PNPI RAS Gatchina, Leningrad district, 188300 Russia.

E-mail: belostot@mail.desy.de, naryshk@mail.desy.de, denis.veretennikov@desy.de

Abstract. Three components of the spin transfer coefficient from the longitudinally polarized electron/positron beam to the Λ or $\bar{\Lambda}$ hyperon have been measured in the HERMES experiment. Kinematical dependencies of the spin-transfer have been studied. Averaged over Λ kinematics, longitudinal component of the spin transfer D_{LL}^{Λ} (along the virtual photon direction) to the Λ hyperon is found to be $D_{LL}^{\Lambda} = 0.19 \pm 0.04_{stat} \pm 0.02_{syst}$.

1. Introduction

Longitudinal spin transfer from a polarized positron to a Λ hyperon produced in the deep-inelastic scattering process is sensitive to two unknowns: the spin structure of the lightest hyperon, and the spin-dependent dynamics of the fragmentation process in deep-inelastic scattering. Given the non-trivial spin structure of the proton [1], it is of interest to consider the spin structure of other baryons.

In the naive Constituent Quark Model the spin of the Λ hyperon is entirely carried by the s quark: $\Delta q_s^{\Lambda} = 1$, while the ud pair is in a spinless (singlet) state, i.e., $\Delta q_u^{\Lambda} = \Delta q_d^{\Lambda} = 0$. Here $\Delta q_f^{\Lambda} \equiv q_f^{\Lambda+} - q_f^{\Lambda-}$, where $q_f^{\Lambda+}$ and $q_f^{\Lambda-}$ are the probabilities to find a quark with the spin parallel or anti-parallel to the the hyperon spin direction, respectively, and q_f^{Λ} ($f = u, d, s$) is the number density for quarks plus antiquarks of flavor f in the Λ hyperon, while the unpolarized number density is $q_f^{\Lambda} \equiv q_f^{\Lambda+} + q_f^{\Lambda-}$.

Alternatively, one can use SU(3)-flavor symmetry in conjunction with the experimental results on the proton to estimate the first moments of the helicity-dependent quark distributions in the Λ hyperon. Using such assumptions Burkardt and Jaffe found $\Delta q_u^{\Lambda} = \Delta q_d^{\Lambda} = -0.23 \pm 0.06$ and $\Delta q_s^{\Lambda} = 0.58 \pm 0.07$ [2]. According to this estimate, the spins of the u and d quarks and antiquarks are directed predominantly opposite to the spin of the Λ hyperon resulting in a weak but non-zero net polarization. If such an SU(3)-flavor rotation (see Eq. 3 of Ref. [3], for example) is applied to the recent semi-inclusive data on the nucleon [4], the values $\Delta q_u^{\Lambda} = \Delta q_d^{\Lambda} = -0.09 \pm 0.06$ and $\Delta q_s^{\Lambda} = 0.47 \pm 0.07$ are obtained instead, favoring a much smaller polarization of the u and d quarks and antiquarks. A lattice-QCD calculation [3] also finds small light-quark polarizations, $\Delta q_u^{\Lambda} = \Delta q_d^{\Lambda} = -0.02 \pm 0.04$ and $\Delta q_s^{\Lambda} = 0.68 \pm 0.04$.

Finally, other authors [5, 6, 7] have employed phenomenological models to explore the dependence of $\Delta q_f^{\Lambda}(x)$ on the Bjorken scaling variable x. These models predict a large positive polarization of the u and d quarks in the kinematic region $x > 0.3$.

Longitudinal spin transfer to Λ hyperon has previously been explored by the LEP experiments OPAL and ALEPH at an energy corresponding to the Z^0 pole [8, 9]. In these experiments the Λ hyperon are predominantly produced via the decay $Z^0 \to s\bar{s}$, in which the primary strange quarks from the decay are strongly (and negatively) polarized at the level of -91%. The OPAL and ALEPH data show a Λ polarization of about -30% at $z > 0.3$.

2. Longitudinal spin transfer

The polarization of final-state Λ hyperon can be measured via the weak decay channel $\Lambda^0 \to p\pi^-$ through the angular distribution of the final-state particles:

$$\frac{dN}{d\Omega_p} = \frac{dN_0}{d\Omega_p}(1 + \alpha\, \vec{P}^{\Lambda} \cdot \vec{k}_p). \tag{1}$$

Here, $\vec{k}_p$ is the unit vector along proton momentum, $\vec{P}^{\Lambda}$ is the polarization of the Λ, and $\alpha = 0.642 \pm 0.013$ is the analyzing power of the parity-violating weak decay. The symbols $dN/d\Omega_p$ and $dN_0/d\Omega_p$ denote the distributions for the decay of polarized and unpolarized Λ samples, respectively. Because of the parity-violating nature of this decay, the proton is preferentially emitted along the spin direction of its parent, thus offering access to spin degrees of freedom in the deep-inelastic scattering final state.

The dominant mechanism for semi-inclusive production of longitudinally polarized Λ hyperon in polarized DIS is sketched in Fig. 1. The process depicted corresponds to Λ production in the current fragmentation domain of the struck quark.

A longitudinally-polarized electron or positron emits a polarized virtual photon γ^* which is absorbed by a quark of opposite spin direction in the target proton. As indicated by the arrows in Fig. 1, this fixes the spin orientation of the struck quark: after the spin-1 photon is absorbed, the outgoing quark has the same helicity as the virtual photon.

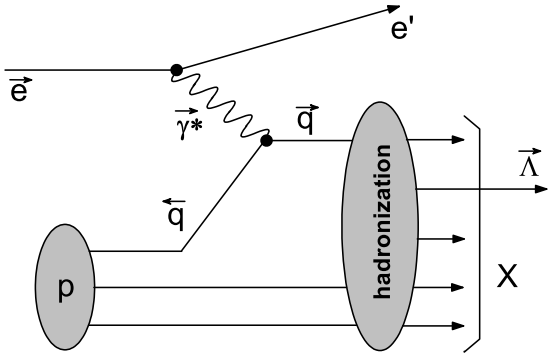

Figure 1. The single-quark scattering mechanism leading to Λ production in the current fragmentation region of polarized deep inelastic electron scattering.

If the longitudinal polarization of the beam is given by P_b and the target is unpolarized, the struck quark will acquire a polarization $P_q = P_b D(y)$. Here $D(y) = [1 - (1-y)^2]/[1 + (1-y)^2]$ gives the depolarization of the virtual photon as compared to the incident electron. Positive beam polarization P_b refers to the case when the beam has positive helicity in the target rest frame. The component of the polarization transferred along the direction L' from the virtual photon to the produced Λ is given by

$$P^{\Lambda}_{L'} = P_b D(y) D^{\Lambda}_{LL'}, \tag{2}$$

where L is the primary quantization axis, directed along the virtual photon momentum and $D^{\Lambda}_{LL'}$ is the spin transfer coefficient describing the probability that the polarization of the struck quark is transferred to the Λ hyperon along a secondary quantization axis L'.

3. The HERMES experiment and data selection

The Λ data were accumulated by the HERMES experiment at DESY. In this experiment, the 27.6 GeV longitudinally-polarized lepton beam [10] of the HERA *e-p* collider passes through an open-ended tubular storage cell into which polarized or unpolarized target atoms in undiluted gaseous form are continuously injected. The HERMES detector is described in detail in Ref. [11].

The data presented here were recorded using elctron/positron beams during: 1996-2007 years. A variety of unpolarized target gases were used in the analysis. Most of the data were collected from hydrogen and deuterium, but ^{3}He, ^{4}He, ^{14}N, ^{20}Ne, ^{84}Kr and ^{132}Xe targets were also included, and the data from all targets were combined. An average beam polarization of about 50% was typical during data taking.

The scattered lepton and the Λ decay products were detected by the HERMES spectrometer in the polar-angle range from 40 to 220 mrad. A positron trigger was formed from a coincidence between three scintillator hodoscope planes and a lead-glass calorimeter. The trigger required a minimum energy deposit in the calorimeter of 3.5 GeV for the data employed in this analysis.

The Λ hyperon were identified in the analysis through their $p\pi^-$ decay channel. Events were selected by requiring the presence of at least three reconstructed tracks: a lepton track and two hadron candidates of opposite charge. If more than one positive or negative hadron was found in one event, all possible combinations of positive and negative hadrons were used. The requirements $Q^2 > 0.8$ GeV^2 and $W > 2$ GeV, where $-Q^2$ is the four-momentum transfer squared of the exchanged virtual photon and W is the invariant mass of the photon-nucleon system, were imposed on the positron kinematics to ensure that the events originated from the deep-inelastic scattering domain. In addition, the requirement $y = 1 - E'/E < 0.85$ was imposed to exclude the large contribution of radiative corrections.

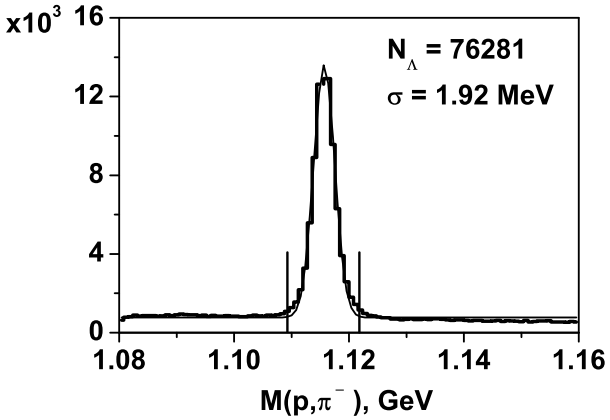

Figure 2. Invariant mass spectra for Λ for the whole data sample of selected events.

Two spatial vertices were reconstructed for each event by determining the intersection (i.e., point of closest approach) of pairs of reconstructed tracks. The primary (production) vertex was determined from the intersection of the beamline and the scattered beam lepton, while the secondary (decay) vertex was determined from the intersection of the proton and pion tracks. For the first (production) vertex, the distance of closest approach was required to be less than 1.5 cm and for second (decay) vertex used vertex probability cut based on improved track reconstruction method. For tracks fulfilling these requirements the invariant mass of the hadron pair was evaluated, under the assumption that the high-momentum leading hadron is the proton while the low-momentum hadron is the pion. In order to suppress the background from hadrons emitted from the the primary vertex, a vertex separation requirement for distant between vertexes $D(v_1, v_2) > 10$ cm has been applied. In addition to that a RICH (or Čerenkov)

based particle identification has been used for reject leading pion. Invariant mass Λ spectra with all the restrictions (above) imposed are shown in Fig. 2 and contain 76280 Λs.

4. Experimental results

4.1. Extraction of $D^{\Lambda}_{LL'}$

Direction of the longitudinal Λ polarization L' is difficult to predict from general principles. It is commonly assumed that the spin is transferred either along the Λ momentum or along the momentum of virtual photon, or along the momentum of primary lepton beam [12, 13, 14, 15]. On the other hand, all three components of the Λ polarization vector can be extracted from the experimental data set. As well as in one-dimension case, extraction of the three component spin-transfer $D^{\Lambda}_{LL'}$ is based on moment method [15]. We rewrite Eq. 2 in vector form:

$$\vec{P}^{\Lambda} = \vec{D}^{\Lambda}_{LL'} D(y) P_b, \tag{3}$$

where vector $\vec{D}^{\Lambda}_{LL'}$ has three components: D^{Λ}_{Lx}, D^{Λ}_{Lx} and D^{Λ}_{Lx}. [1]

The direct product $\vec{P}^{\Lambda} \cdot \vec{k}_p$ can be written as $D(y)P_b(D^{\Lambda}_{Lx}\cos\theta_x + D^{\Lambda}_{Ly}\cos\theta_y + D^{\Lambda}_{Lz}\cos\theta_z)$, where θ_x, θ_y and θ_z are the angles between the proton momentum and x, y and z axes of a Cartesian coordinate system, respectively. A detailed derivation based on the moment method leads to the following equations:

$$\sum_{k=x,y,z} D^{\Lambda}_{Lk} A_{i,k} = \frac{1}{\alpha} \frac{B_i}{\|P_b^2\| - \|P_b\|^2}, (i = x, y, z). \tag{4}$$

Here $A_{i,k} = \left\langle \frac{D^2(y)\cos\theta_k \cos\theta_i}{1+\alpha\|P_b\|D(y)\sum_j D^{\Lambda}_{Lj}\cos\theta_j} \right\rangle$ and $B_i = \langle P_b D(y)\cos\theta_i - \|P_b\|D(y)\cos\theta_i\rangle$ represent average over experimental Λ data set of selected N_Λ events,(i.e. $\langle ... \rangle = \frac{1}{N_\Lambda}\sum_{m=1}^{N_\Lambda} ...$) while $\|P_b\| = \frac{1}{L}\int P_b dL$, $\|P_b^2\| = \frac{1}{L}\int P_b^2 dL$ represent luminosity-weighted P_b and P_b^2. It is easy to see that $A_{i,k} = A_{k,i}$ and ,moreover, matrix $\widehat{A}$ is practically diagonal.

For a helicity balance data set ($\|P_b\| = 0$) Eq. 4 is reduced to a system of linear equations from which three components of $\vec{D}^{\Lambda}_{LL'}$ can be directrly extracted and taken as a result of first iteration. As long as the beam polarization changes periodically its sign, the factor in denominator of $A_{i,k}$ proportional to $\|P_b\|$ is typically small. This small correction may be calculated using D^{Λ}_{Lj} $j = x, y, z$, from the first iteration and iteration procedure should be repeated. In practice, the iteration chain converges very fast so that after three iteration steps D^{Λ}_{Lj} is found with a good enough accuracy.

4.2. Coordinate systems and $D^{\Lambda}_{LL'}$ averaged over experimental data set.

In the Λ rest frame, introduce two Cartesian coordinate systems (Fig. 3):

(i) z-axis is along virtual photon momentum $\vec{p_\gamma}$, y-axis is perpendicular to the plane formed by the virtual photon momentum $\vec{p_\gamma}$ and the vector in direction of Λ momentum $\vec{p_\Lambda}$ (not affected by the relativistic transformation to the Λ rest frame), x-axis is perpendicular to the zy-plane;

(ii) z'-axis is along the direction of Λ momentum $\vec{p_\Lambda}$, y'-axis is perpendicular to the plane formed by the virtual photon momentum $\vec{p_\gamma}$ and the Λ momentum $\vec{p_\Lambda}$, x'-axis is perpendicular to the $z'y'$-plane.

All three components of spin transfer $D^{\Lambda}_{LL'}$ have been reconstructed using both coordinate system (i and ii). The results are presented in Tab. 1 and schematically shown in Fig. 4 and Fig. 5.

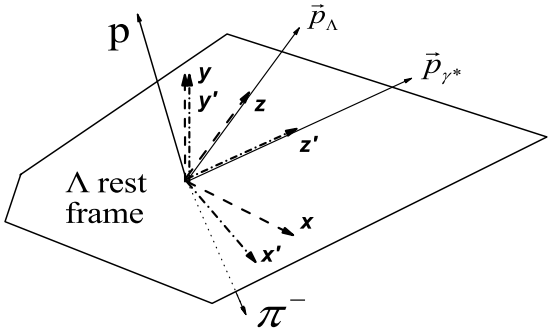

Figure 3. Sketched view of coordinate systems in Λ rest frame.
$\vec{k}_z = \vec{p}_\Lambda$, $\vec{k}_y = \vec{p}_\Lambda \times \vec{p}^*_\gamma$, $\vec{k}_x = \vec{k}_y \times \vec{k}_z$,
$\vec{k}_z = \vec{p}^*_\gamma$, $\vec{k}_y = \vec{p}_\Lambda \times \vec{p}^*_\gamma$, $\vec{k}_x = \vec{k}_y \times \vec{k}_z$

Table 1. Measured values of $D^\Lambda_{LL'}$.

Component	z axis along virtual photon $\vec{p}_{\gamma^*}$	z axis along $\vec{p}_\Lambda$
D^Λ_{Lx}	$-0.016 \pm 0.042_{stat} \pm 0.017_{syst}$	$0.133 \pm 0.039_{stat} \pm 0.015_{syst}$
D^Λ_{Ly}	$0.037 \pm 0.037_{stat} \pm 0.017_{syst}$	$0.037 \pm 0.037_{stat} \pm 0.017_{syst}$
D^Λ_{Lz}	$0.186 \pm 0.040_{stat} \pm 0.012_{syst}$	$0.147 \pm 0.038_{stat} \pm 0.015_{syst}$
$D^\Lambda_{LL'}$	$0.187 \pm 0.040_{stat} \pm 0.017_{syst}$	$0.197 \pm 0.039_{stat} \pm 0.017_{syst}$

For HERMES kinematics, unlike the case of DIS at very high energies, axes z and z' are not collinear. From one event to another, the angle between z and z' axis varies over a wide range with an average value of 35 degrees. By that reason, the values of $D^\Lambda_{LL'} = \sqrt{(D^\Lambda_{Lx})^2 + (D^\Lambda_{Lx})^2 + (D^\Lambda_{Lx})^2}$ found for two coordinate systems are not exactly equal one to another. This discord becomes negligibly small in the case of infinite statistics ($1/N_{Lambda} \to 0$).

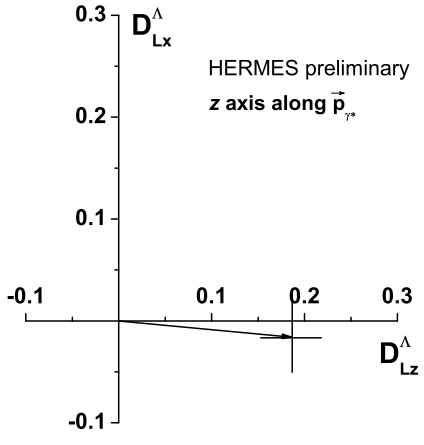

Figure 4. Two dimensional plots for integrated $D^\Lambda_{LL'}$, z axis along virtual photon $\vec{p}_{\gamma^*}$.

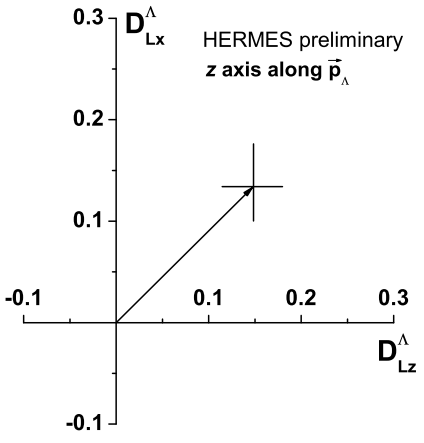

Figure 5. Two dimensional plots for integrated $D^\Lambda_{LL'}$, z axis along $\vec{p}_\Lambda$.

[1] Note that vector $\vec{D}^\Lambda_{LL'}$ is defined in the Λ rest frame and thus given in nonrelativistic form.

One can see from Table 1 that the component D^{Λ}_{Ly} of spin transfer is compatible with zero within statistical and systematical uncertainties as it must be because of parity conservation requirement.

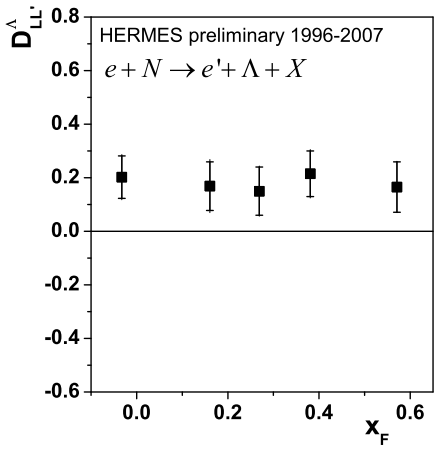

Figure 6. $D^{\Lambda}_{LL'}$ versus x_F.

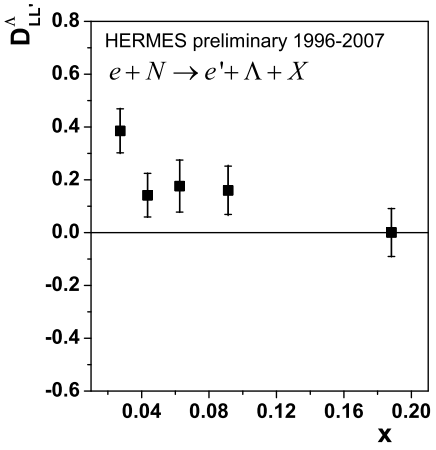

Figure 7. $D^{\Lambda}_{LL'}$ versus x.

One may also conclude that the spin transferred practically along the virtual photon momentum. In the frame of single-quark scattering mechanism shown on Fig. 1. this would mean that the struck quark preserves the helicity of the virtual photon in the fragmentation process resulted in Λ formation.

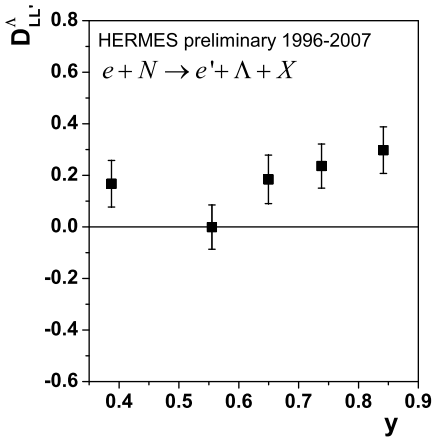

Figure 8. $D^{\Lambda}_{LL'}$ versus y.

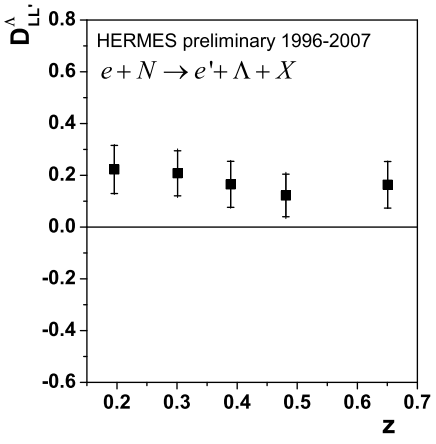

Figure 9. $D^{\Lambda}_{LL'}$ versus z.

Below all dependencies are plotted only for D^{Λ}_{Lz} for the case, when z axis is along virtual gamma direction $\vec{p}_{\gamma^*}$. D^{Λ}_{Lx} and D^{Λ}_{Ly} are also calculated and controlled, but for all bins for all dependencies its compatible with zero.

4.3. Dependence of $D^{\Lambda}_{LL'}$ on kinematic variables.
Distributions over DIS kinematical variables are displayed in Figs. 6, 7, 8, 9.

Kinematical behavior of $D^{\Lambda}_{LL'}$ shows the dependence on x while x_F, y and z dependencies looks practically flat.

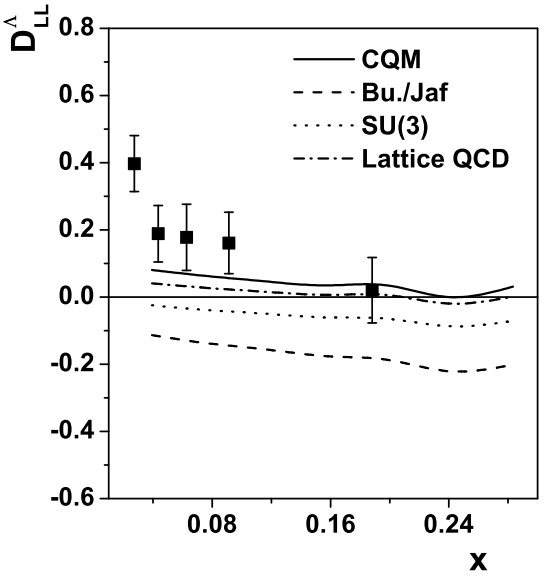

Figure 10. Theoretical model prediction.
Constituent quark model (CQM)
$\Delta u = \Delta d = 0, \Delta s = 1$
Burkard/Jaffe
$\Delta u = \Delta d = -0.23 \pm 0.06, \Delta s = 0.58 \pm 0.07$
SU(3) flavor symmetry
$\Delta u = \Delta d = -0.09 \pm 0.06, \Delta s = 0.47 \pm 0.07$
Lattice QCD
$\Delta u = \Delta d = -0.02 \pm 0.04, \Delta s = 0.68 \pm 0.04$.

The spin transfer can be rewritten as $D^{\Lambda}_{LL'} = \sum_f D^{\Lambda}_{LL',f}\omega^{\Lambda}_f$, where $D^{\Lambda}_{LL',f}$ denotes the partial spin transfer from a struck quark of favor f to a Λ hyperon and purity ω^{Λ}_f is the net probability that a Λ was produced after absorption of a virtual photon by a quark of favor f [15]. Under the assumptions that the produced hyperon actually contains the struck quark of favor f, that it was produced directly from fragmentation (and not from the decay of a heavier hyperon), and that the original helicity of the quark is preserved during the fragmentation process, the partial spin-transfer coefficient has been estimated using a theoretical model of the Λ spin structure to be [16] $D^{\Lambda}_{LL',f} \simeq \frac{\Delta q^{\Lambda}_f}{q^{\Lambda}_f}$.

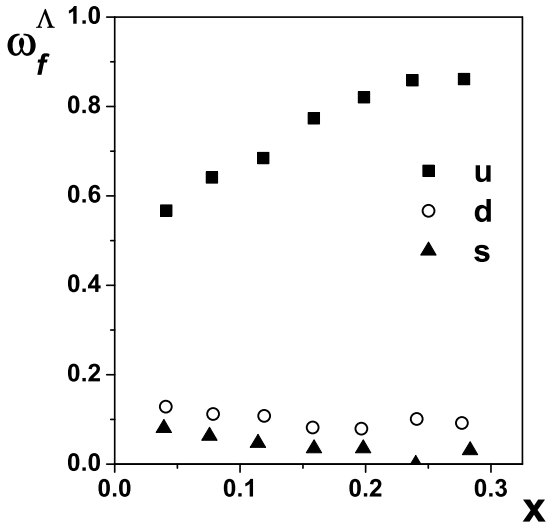

Figure 11. Purities for Λ production from the proton target within the HERMES acceptance

Using such assumptions and purity, which is obtain from Monte-Carlo (see Fig. 11) one can calculate $D^{\Lambda}_{LL'}$. On Fig. 10 the data are presented with the phenomenological model calculations of Ref. [2, 3]. All calculation predict a pronounced rise of the spin transfer at small values of x, but the value of $D^{\Lambda}_{LL'}$ is smaller then the obtained by HERMES. Should be mentioned here that no Λ from hyperon resonances decay (Σ^*, Σ^0, Ξ) is taken in to account for this calculation.

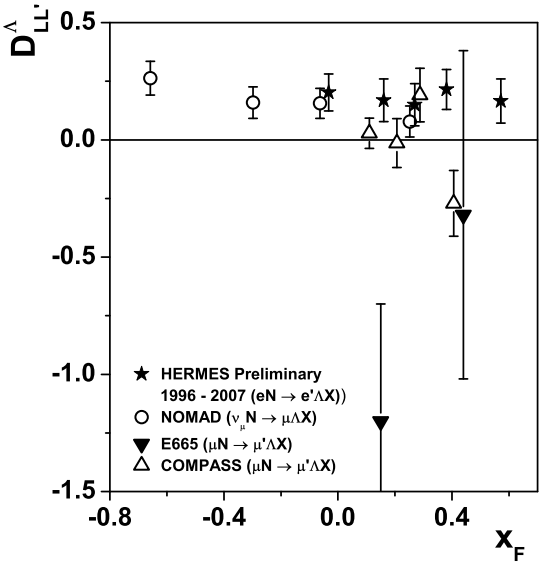

Figure 12. Combination of world data of $D^{\Lambda}_{LL'}$.

In order to provide a comparison with other DIS scattering experiments, and to illustrate the level of agreement in the region of overlap, the HERMES data are shown in Fig. 12 together with data obtained by the NOMAD experiment [17] at CERN with a 43 GeV ν_μ-beam. Results from the Fermilab E665 experiment [18] obtained with a 470 GeV and COMPASS [19] with 200 GeV polarized muon beam are also shown.

As shown in Fig. 12, the NOMAD - HERMES and COMPASS - HERMES results are indeed compatible in the kinematic region of overlap $-0.2 < x_F < 0.3$ and $0.1 < x_F < 0.4$, respectively.

5. Acknowledgments

We gratefully acknowledge the DESY staff and the staffs of the collaborating institutions. This work was supported by the Russian Academy of Science and the Russian Federal Agency for Science and Innovations.

References

[1] B W Filippone and X D Ji, Adv. Nucl. Phys. 26 (2001) 1.
[2] M Burkardt and R L Jaffe, Phys. Rev. Lett. 70 (1993) 2537.
[3] QCDSF Collaboration, M Göckeler et al., Phys. Lett. B 545 (2002) 112.
[4] HERMES Collaboration, A Airapetian et al., Phys. Rev. Lett. 92 (2004) 012005; Phys. Rev. D 71 (2005) 012003.
[5] B Q Ma, J J Yang, I Schmidt, Phys. Lett. B 477 (2000) 107.
[6] C Boros, J T Londergan, and A W Thomas, Phys. Rev. D 61 (2000) 014007.
[7] C Liu and Z Liang, Phys. Rev. D 62 (2000) 094001.
[8] OPAL Collaboration, K Ackerstaff et al., Eur. Phys. J. C 2 (1998) 49.
[9] ALEPH Collaboration, D Buskulic et al., Phys. Lett. B 374 (1996) 319.
[10] D P Barber et al., Phys. Lett. B 343 (1995) 436.
[11] HERMES Collaboration, K Ackerstaff et al., Nucl. Instrum. Methods A 417 (1998) 230.
[12] R L Jaffe, Phys. Rev. D 54, 6581 (1996).
[13] P J Mulders and R D Tangerman, Nucl. Phys. B 461 (1996) 197.
[14] A Kotzinian, A Bravar, D von Harrach Eur. Phys. J. C 2 (1998) 329.
[15] HERMES Collaboration A Airapetian et al., Phys.Rev.D74 (2006) 072004.
[16] D Ashery and H J Lipkin, Phys. Lett. B 469, 263 (1999).
[17] NOMAD Collaboration, P Astier et al., Nucl. Phys. B 588 (2000) 3.
[18] E665 Collaboration, M R Adams et al., Eur. Phys. J. C 17 (2000) 263.
[19] COMPASS Collaboration, M Alekseev et al., Eur. Phys. J. C 64 (2009) 171-179.